The International Journal of Advanced Manufacturing Technology (2019) 102:1913–1921
https://doi.org/10.1007/s00170-018-03226-4

ORIGINAL ARTICLE

High-speed grinding of HIP-SiC ceramics on transformation of microscopic features

Chongjun Wu[1,2] · Jingzhu Pang[1] · Beizhi Li[1] · Steven Y Liang[2]

Received: 10 August 2018 / Accepted: 13 December 2018 / Published online: 15 January 2019

Abstract

Grinding has become one of the most efficient precision machining methods to treat with undesired machining defects and improve the surface integrity for the hard and brittle engineering ceramics. However, it is inevitable to cause micro-damages and related transformation of microscopic features, which will eventually affect the grinding quality. This paper is devoted to investigate the high-speed grinding microscopic features of silicon carbide ceramics to reveal the application of high-speed grinding technique in precision machining of ceramics. A comparative study of high-speed and conventional speed grinding of silicon carbide ceramics is discussed in terms of phase transformation, residual stresses, micro-damages, grinding chips, and surface topography. The results show that the high-speed grinding (HSG) process could help substantially improve the workpiece integrity in terms of better surface finish, smaller damages, and controlled residual stresses with a higher material removal rate. Moreover, it has also been proved that a polytypic phase transformation could be induced in HSG process.

Keywords Microscopic features · High-speed grinding · Engineering ceramics · Grinding damages · Ductile grinding

1 Introduction

Silicon carbide ceramics, such as valves, bearing, rotors and optical instruments [1], have been widely used in engineering industry for the superior performance in hardness and thermal, wear, and chemical resistance. However, the brittle and hard nature is still a big obstacle to restrain the precision mechanical machining and thus a limitation of a broader engineering application. In recent years, grinding with diamond wheels [2–4] has become the most effective method to achieve a satisfying surface integrity with less damage, especially in high-speed grinding (HSG) process. Compared with the conventional grinding (CG) process, HSG process is a much more efficient machining method with a higher wheel speed of more than 60 m/s, which could help to substantially reduce the chip thickness [5] and the grinding force [6] and thus improve the grinding surface texture [7]. Nevertheless, the investigation of ceramic microscopic features under high-speed grinding is obviously insufficient, and more works need to be conducted to promote the application of this technique.

In recent years, some work has been done to investigate the grinding-induced microscopic features of ceramic materials. During the grinding process, the workpiece material will undergo a coupling thermo-mechanical load, which could affect the ground quality in terms of the ground surface textures, phase transformation, and residual stress. It has been proved that the SiC could transform from β-SiC (3C cubic) to α-SiC (4H, 6H hexagonal) under some extreme high temperature or pressure [8–10]. However, there is no reported experimental detail for phase transformation in grinding of SiC. For zirconia ceramics, Frangulyan et al. [11] investigated the post-grinding phase transformation with thermal annealing of the ceramic specimen. On the other hand, the grinding-induced residual stress is also an important indicator to reflect the material inner stress, which could affect materials' service life if not well controlled. In the study of grinding mechanism, the HSG chips were simulated through finite element analysis to reflect the grinding mechanism in grinding of nickel-based super alloy [12]. However, the grinding chips for brittle materials are much more complicated to analyze for the heterogeneous structure and random crack generation. In the subsequent

✉ Jingzhu Pang
pangjz@dhu.edu.cn

[1] College of Mechanical Engineering, Donghua University, Shanghai 201620, China

[2] Manufacturing Research Center, Georgia Institute of Technology, Atlanta 30332, USA

work, the researchers [13–15] established the relationship between the grinding damages and surface roughness, which could help to comprehensively define the surface quality through the process parameters. In study of ceramic grinding textures, Kovach [16] has demonstrated that the HSG could help to reduce surface crack and improve the surface polish. Moreover, the ceramic materials are tended to be removed by a transition from brittle fracture removal to ductile plastic removal [17]. These works, related to the grinding-induced microscopic features, fail to report the "speed effect" in high-speed grinding of ceramics.

Ductile-mode machining was first proposed by King et al. [18] during the observation of some plastic deformation in frictional wear of rock salts. Later on, Lawn et al. [19] establish a critical depth to describe the relationship between load and crack size in indenting hard materials. In the subsequent work, the critical depth for brittle-ductile transition was proposed based on the material removal energy analysis [20]. Based on the critical depth model, more related works [21–24] in ductile grinding were conducted to associate the ductile removal process with material properties [20], tool geometry [21], and even the process parameters [23]. In grinding of BK7 optical glass, the typical damage mechanism was studied in high-speed process [2]. However, for silicon carbide ceramics, the research works are either in micro-machining or conventional speed grinding, which has prevented its broader industrial application for efficiency and quality. Thus, high-speed grinding process for brittle materials needs more clear understanding in its transformation of micro features.

In this paper, grinding experiments were conducted on the HIP-SiC ceramics to reveal the high-speed grinding–induced microscopic features. A comparative study is given to reveal the machining efficiency and surface integrity in HSG process compared with the CG process. This paper will discuss the grinding-induced phase transformation, residual stresses, grinding chips, damages, and other related topography in detail.

2 Materials and methods

In this work, the grinding experiments were conducted on a cylindrical high-speed grinder MGKS1332/H (Shanghai Machine Tool Inc.) with a linear speed of up to 150 m/s. The experimental setup is illustrated in Fig. 1a. The grinding wheel was installed with a wheel balancing system (SBS model SB 4500), which was used to dynamically balance the grinding wheel spindle under 0.03 μm before each test. In this paper, a 5% water-soluble metal cutting fluid and vitrified diamond wheel (D91 V + 2046J1SC C150E, Φ400 × 22 × 203.5) will be used in the experiment. The grinding wheel was trued by a diamond-truing wheel at a speed ratio of 0.8 under a cutting depth of 2 μm, wheel speed of 80 m/s, and the transverse feedrate of 400 mm/min. In addition, the grinding temperature was detected through a K-type grindable thermocouple, which is connected with a NI-USB 9213 card and Labview acquisition software on a laptop. The thermocouple metal wires were first planished to improve the contact area of the hot end, and then inserted into the workpiece groove as shown in Fig. 1b. The calibration is conducted in a furnace under a temperature of 100–800 °C, which shows an error below 1 °C. The detailed experimental conditions are listed in Table 1.

The workpiece material is hot isostatic pressing silicon carbide (HIP-SiC), whose mechanical properties could be found in Table 2. In this paper, β-SiC powders were pressed at a pressure of 200 MPa and temperature of 1850 °C for 1 h with additives B and C. The workpiece specimen which could be seen in Fig. 1 b and c is the polished surface. The

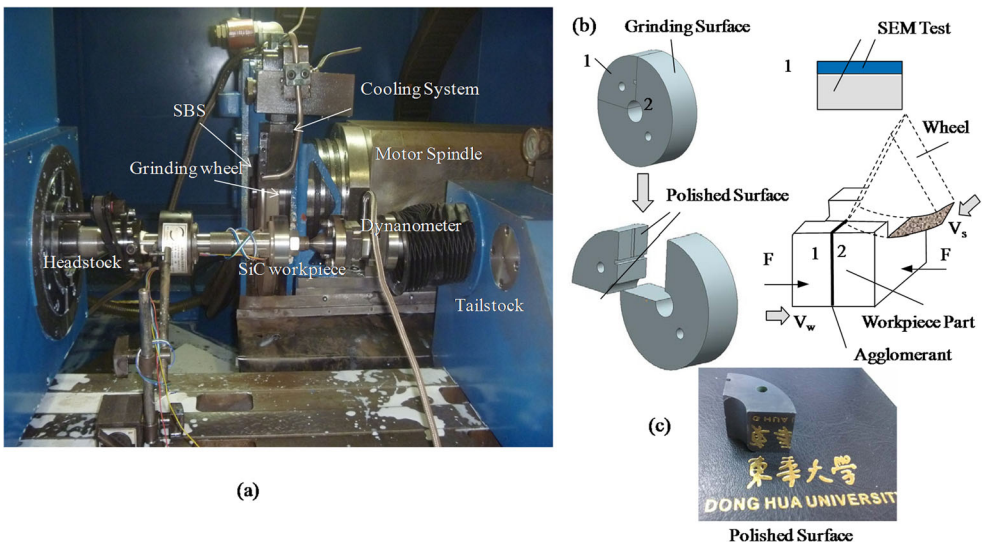

Fig. 1 Experiments setup (a) the grinding platform; (b) workpiece details; (c) polished surface

Table 1 Experimental conditions

Title	Specification	Title	Specification
Grinding machine	CNC cylindrical grinding machine MGKS1332/H	Wheel spindle balancing system	SBS model SB-4500 below 0.03 μm
Grinding wheel	Vitrified diamond wheel D91 V+ 2046 J1SC-23 C150 E	Coolant	Water-based emulsion 5% (10 L/min)
Mode	Up grinding	Depth of cut	1–20 μm
Wheel speed	20–80 m/s	Workpiece speed	300–1200 mm/min

specimen has a width of 20 mm and diameter of 60 mm. The workpiece was first divided into two parts as shown in Fig. 1b. The side face of the minor part was polished with diamond paste from 40 to 0.5 μm for the SEM test. Before XRD and SEM test, the ground specimen was ultrasonic bathed in acetone liquid for 15 min.

In this paper, the x-ray diffraction (XRD) was detected on a Rigaku D/max 2550 V (Japan) with a Cu Kα radiation. The step angle is 0.02°. However, the residual stress was measured through a Proto LXRD (Canada) with Cu Kα radiation, which could detect 7 different diffraction data with 2 detectors and then calculate the residual stress at a low calculation error of less than 20 Mpa. The surface/subsurface topography and grinding chips were examined by an environment scanning electron microscope (ESEM) QUANTA 250 from Czech. Finally, the surface roughness was measured through a 3-D Bruker Nano Surface white light interferometer (Npflex).

3 Results and discussions

3.1 XRD analysis

The XRD data was given in Fig. 2 through professional XRD analysis software Jade 6.5. In this figure, ② and ③ represents the conventional speed and high-speed grinding process, while ④ is the XRD data before experiments. ① is the fitting curve of XRD data ④ based on Pearson VII distribution. The fitting error R for ②, ③, and ④ is 9.46%, 8.74%, and 11.24%. The v_s represents the wheel speed, v_w is the workpiece rotational speed, and a_p is the depth of cut. As the material removal rate can be given as $Q'_w = v_w * a_p$, thus the materials' removal rate in ② and ③ are equal. The reference files and Bragg positions for different polytypes are given in the lower part of Fig. 2. Figure 3 is the compositional ratio of various polytypes at different grinding patterns. The relative composition ratios of different polytypes are calculated by the reference intensity ratios (i.e., RIR) through the commercial software Jade 6.5. It can be found that the β-SiC is the main composition before experiments, which could reach up to 78.3%. However, when it is in the conventional grinding of 20 m/s, the β-SiC drops down to 14.5%, while the α-SiC consists of 39.9% of 4H-SiC and 45.6% 6H-SiC. While in high-speed grinding of 80 m/s, the β-SiC takes up 43.8%, which is much higher than the conventional grinding. Moreover, the α-SiC becomes a 13.6% of 4H-SiC and 42.6% of 6H-SiC.

From the above analysis, it could be concluded that grinding process has induced the phase transformation of SiC ceramics. In high-speed grinding, a minor phase transformation happened and the 6H-SiC almost stay the same with the conventional grinding. While in the conventional grinding, a lower β-SiC and higher 4H-SiC can be found, which means that more phase transformation happens in the conventional grinding than high-speed grinding.

The reason for the phase transformation may be due to the grinding-induced shock temperature and pressure, which has been proved by Zhu et al. [8] through shock wave recovery experiments of a gun shooting. The grinding temperature for the SiC ceramics can be found in Fig. 4, which gives the typical shock temperature rise of grinding temperature. However, the real temperature should be lower than the real grinding temperature for the thermal conduction and scattering into the air, workpiece, wheel, and coolants. Moreover, the same shock pressure characteristics could be found in the grinding forces, which could produce a strain rate up to 10^{-5}–10^{-7}/s in the grit-workpiece scratching process and thus

Table 2 Mechanical properties for SiC

SiC properties						
	Density	3-point bending strength	Vickers hardness	Palmqvist fracture toughness	Elastic modulus	Poisson rate
	ρ_{SiC}	σ_b	H_v	K_{1C}	E_{SiC}	μ_{SiC}
	(g/cm3)	(MPa)	(GPa)	(MPa.m1/2)	(GPa)	(−)
SiC	3.22	490	23	3.5	410	0.16

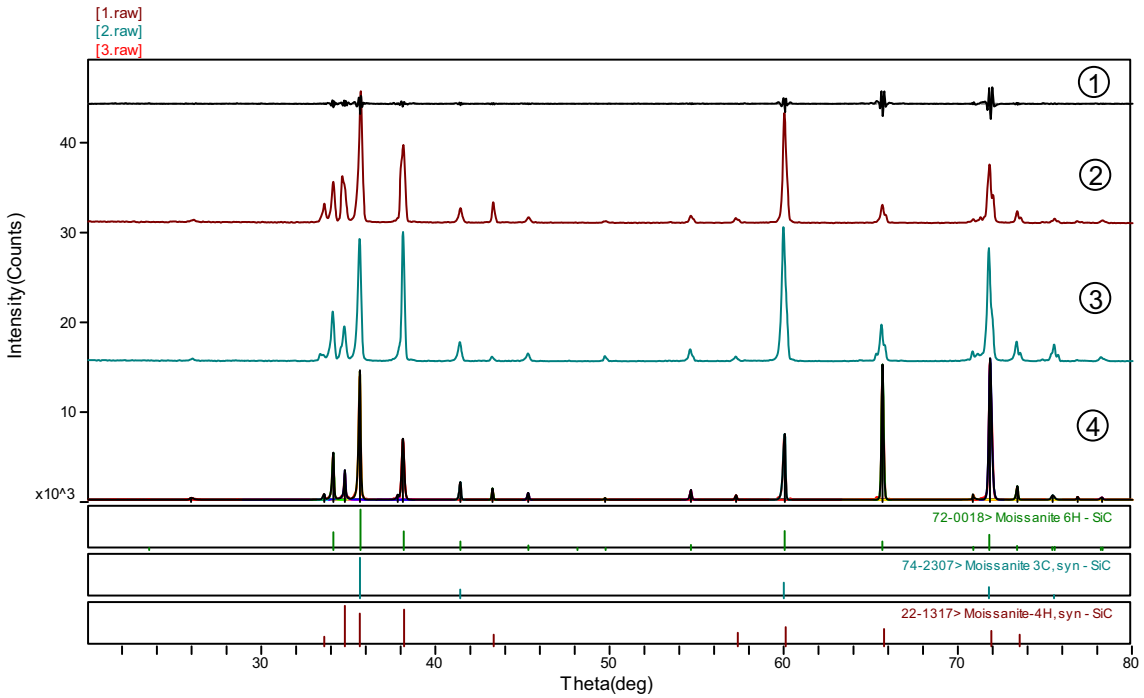

Fig. 2 XRD for SiC. ① Fitting curve of ④. ② CG at $v_s = 20$ m/s, $v_w = 0.067$ m/s, and $a_p = 15$ μm. ③ HSG at $v_s = 80$ m/s, $v_w = 0.267$ m/s, and $a_p = 3.8$ μm. ④ Before experiments.

lead a higher hardness polytype β-SiC. Yet, this explanation still needs further theoretical and engineering verification, which would be a major scientific focus.

3.2 Residual stresses

The residual stress is the material inner stress induced by grinding process. A good understanding of residual stress could help to control the machining-induced stress, which could further improve the grinding quality and the component's service life. In order to analyze the grinding mechanism, the maximum chip thickness h_{cu} is given as formula (1) [25]. The maximum chip thickness is the theoretical chip thickness to define the grinding process.

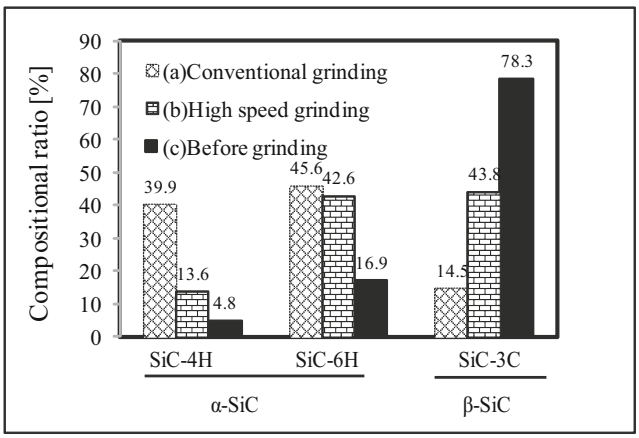

Fig. 3 The compositional ratio of polytypes at different grinding patterns

$$h_{cu} = \left(\frac{3}{C_d{}^{*}\tan\theta} * \frac{v_w}{V_s} * \sqrt{\frac{a_p}{d_e}}\right)^{\frac{1}{2}} \quad (1)$$

where C_d is the active grits number in unit area, θ is the semi-included angle of grit, d_e is the equivalent wheel diameter, $d_e = d_s{}^{*}d_w/(d_s + d_w)$, d_w is the workpiece diameter, and d_s is the wheel diameter.

In Fig. 5, the wheel speed effect on the residual stresses is depicted. It can be found from Fig. 5a that, with the increase of wheel speed, the stress both perpendicular and parallel to the grinding direction becomes lower, almost 30% reduction. This could be explained from formula (1) that the increase of wheel speed v_s will lead to a smaller chip thickness, thus a reduction of grinding force. Moreover, a lower grinding force causes minor grinding damage. Therefore, the inner residual stress could be alleviated through the increase of wheel speed. However, a combination of the increase of workpiece speed and decrease of depth of cut in Fig. 5b causes a relatively stable residual stress, as the chip thickness in formula (1) remains steady, which helps to balance the induced grinding force [22]. In this circumstance, the increase of workpiece speed and decrease of depth of cut could substantially increase the grit-workpiece interaction speed, which could cause shocked lateral and radial cracks generated and partial unstable residual stress in both the perpendicular and parallel direction, such as the workpiece speed of 0.8 m/s. Moreover, it can be found in formula (1) that the variation of both v_w and a_p could lead to uncertain variation of chip thickness, which could cause this residual stress abnormalcy.

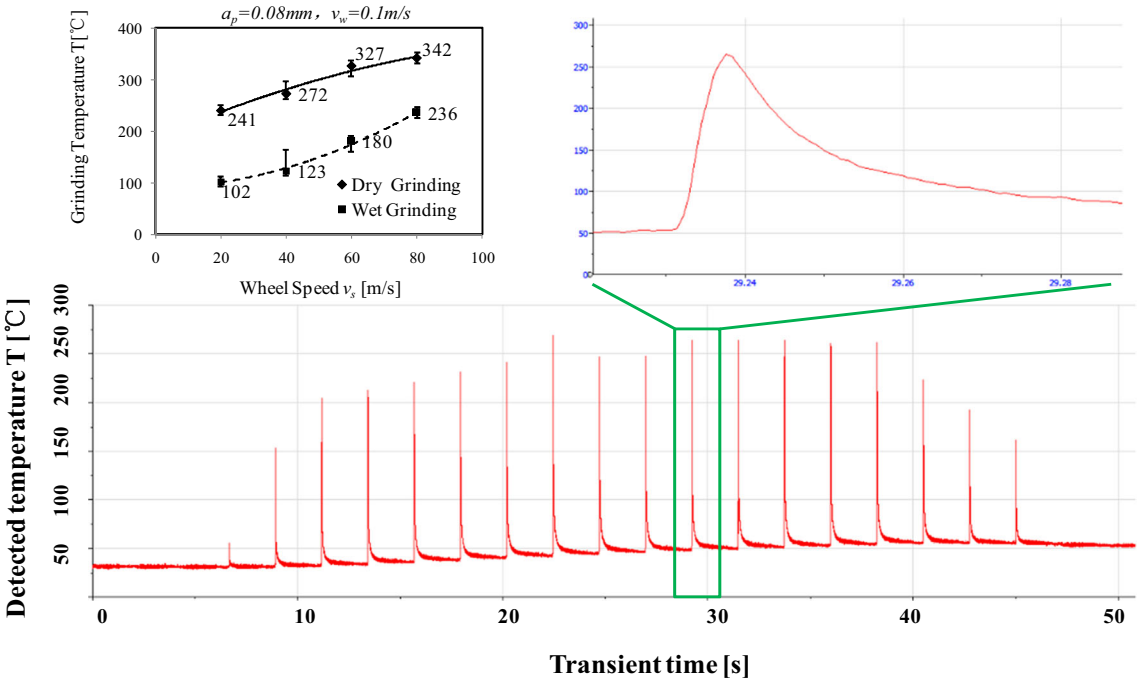

Fig. 4 Grinding temperature characteristics

In Fig. 6, the speed ratio v_s/v_w and depth of cut keep constant; the material removal rate increases substantially as the workpiece speed increases. Under this circumstance, with the increase of wheel speed, the residual stresses slightly increase of about 30%, while the materials' removal rate increases about 4 times. That is to say, a higher grinding speed with fast feed rate could help substantially improve the grinding efficiency without causing a huge effect on residual stresses. As the workpiece speed increase substantially, the same phenomenon of unstable perpendicular and parallel residual stress could be found as Fig. 5b illustrated. From the residual stress data in Figs. 5 and 6, the most prominent conclusion can be found that the perpendicular stress is generally higher than the parallel stress, which could be explained by the lateral crack generation mechanism of brittle materials [7, 19].

3.3 Grinding damages

The grinding damages can be observed through the SEM microscopic pictures. The ground surface SEM was given in Fig. 7. Figure 7a and b represent the conventional grinding and high-speed grinding, respectively. In brittle materials grinding, ductile grinding, which is generally characterized by surface plastic strips caused by plastic deformation energy [7, 20], has been an effective process method to reduce the crack generation. It can be found that the ground surface in Fig. 7 has massive fracture cracks and caves in CG process, while less plastic deformation occurs. However, when it is under HSG process in Fig. 7b, the ground surface was characterized by more plastic deformation, and the fracture cracks become smaller. It has been commonly accepted that the elevation of grinding speed could help to inhabit the grinding cracks [2, 15].

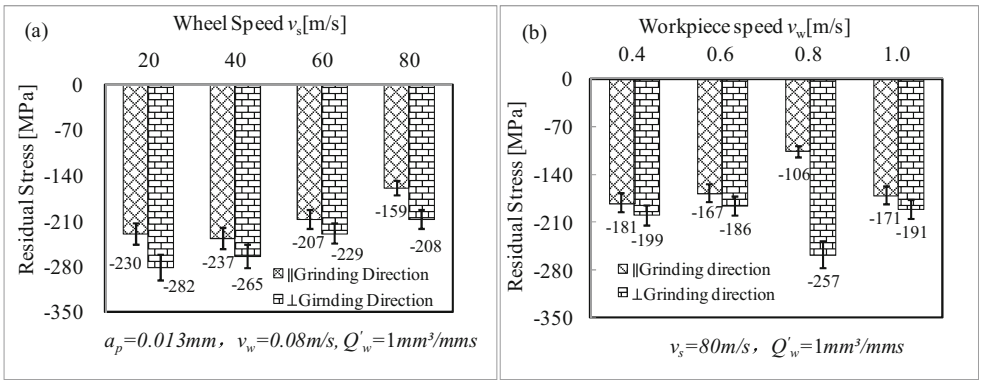

Fig. 5 Speed effect on residual stresses

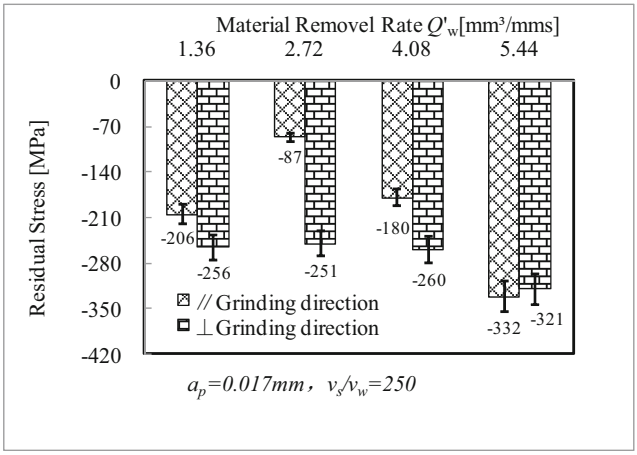

Fig. 6 Residual stresses with high efficiency at HSG

Therefore, it can be concluded that the HSG process could produce more plastic deformation and the material will be more tended to ductile grinding with less fracture cracks. This is attributed to typical speed effect. In HSG process, the increase of grinding wheel speed lead to a combined action of strain rate increase and chip thickness reduction, which helps to restrain the crack propagation.

The ground subsurface SEM is given in Fig. 8. It can be found from the ground SEM pictures that a huge fracture crack with a 65-μm damage depth was produced in CG process of Fig. 8a. However, it is only 14 μm in HSG process and few cracks produced in Fig. 8b. Therefore, the HSG process could also help to reduce the subsurface damage. This could also be explained from the grinding surface damage reduction in Fig. 7.

From the surface and subsurface damage features, the phase transformation could help to explain this phenomenon. As is known by researchers, the β-SiC, a cubic crystal structure, has a much higher hardness than hexagonal crystal structure α-SiC, which is obviously caused by "speed effect" that substantially increase the shock strain rate in HSG.

3.4 Ductile grinding features

In order to reveal more grinding features, the grinding chips and surface roughness are given in this section. The grinding chips are given with SEM pictures in Fig. 9. It can be found that the grinding chips in CG process show a typical brittle fracture feature in Fig. 9a compared with distinct ductile feature in Fig. 9b of HSG process. In Fig. 9b, the ground surface is more characterized by plastic stripes and few fracture cracks in the surface, the upheaved materials are much more smooth, and fine surface could be found. This could also be verified by some simulation work [2, 15] and grinding surface [26] in high-speed grinding of metallic materials.

Figure 10 illustrates the grinding surface roughness under CG and HSG process. Figure 10 a and c are under the same chip thickness of 1.04 μm, while Fig. 10 b and d are 0.52 μm. It can be found from Fig. 10 a and c that the increase of wheel speed from 20 to 80 m/s help substantially reduce the surface roughness from 0.541 to 0.317 μm. Moreover, the surface caves become

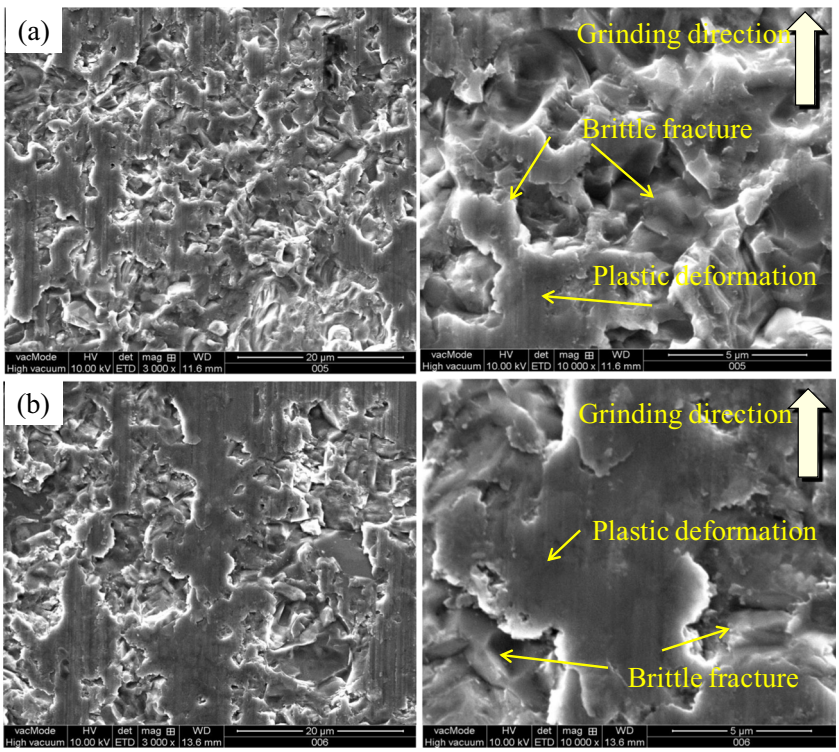

Fig. 7 Surface SEM. **a** CG at v_s = 20 m/s, v_w = 0.067 m/s, and a_p = 15 μm. **b** HSG at v_s = 80 m/s, v_w = 0.267 m/s, and a_p = 3.8 μm. The right pictures are partially enlarged pictures

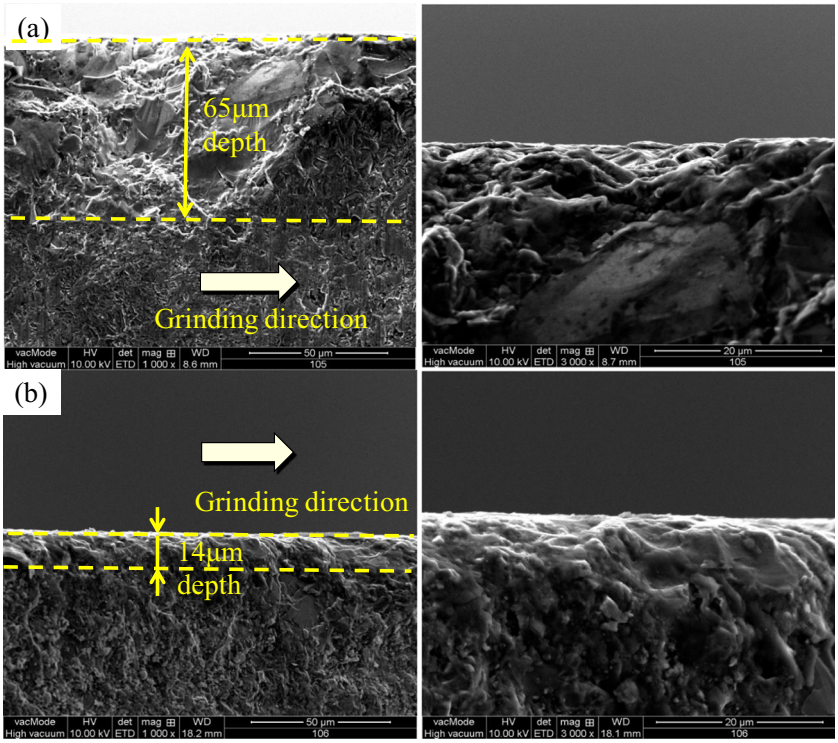

Fig. 8 Subsurface SEM. **a** CG at $v_s = 20$ m/s, $v_w = 0.067$ m/s, and $a_p = 15$ μm. **b** HSG at $v_s = 80$ m/s, $v_w = 0.267$ m/s, and $a_p = 3.8$ μm. The right pictures are partially enlarged pictures

lesser and smoother. On the other hand, it can be found from Fig. 10 a and b that a smaller chip thickness h_{cu} could help to reduce the surface roughness and the surface finish become better. Thus, it can be concluded that the increase of wheel speed and reduction of chip thickness will lead to a better surface finish and lesser fracture surface will be produced. This could be a complementary verification of "speed effect" for not only merely increase of workpiece speed [15, 27] but also an elevation of wheel speed.

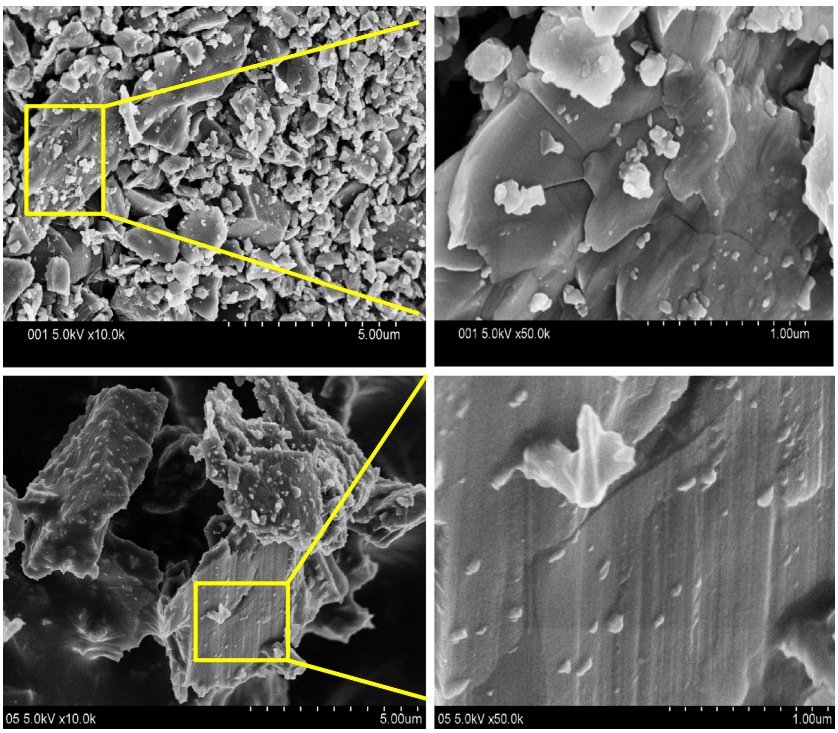

Fig. 9 Grinding chips SEM. **a** CG at $v_s = 20$ m/s, $v_w = 0.067$ m/s, and $a_p = 15$ μm. **b** HSG at $v_s = 80$ m/s, $v_w = 0.267$ m/s, and $a_p = 3.8$ μm. The right pictures are partially enlarged pictures

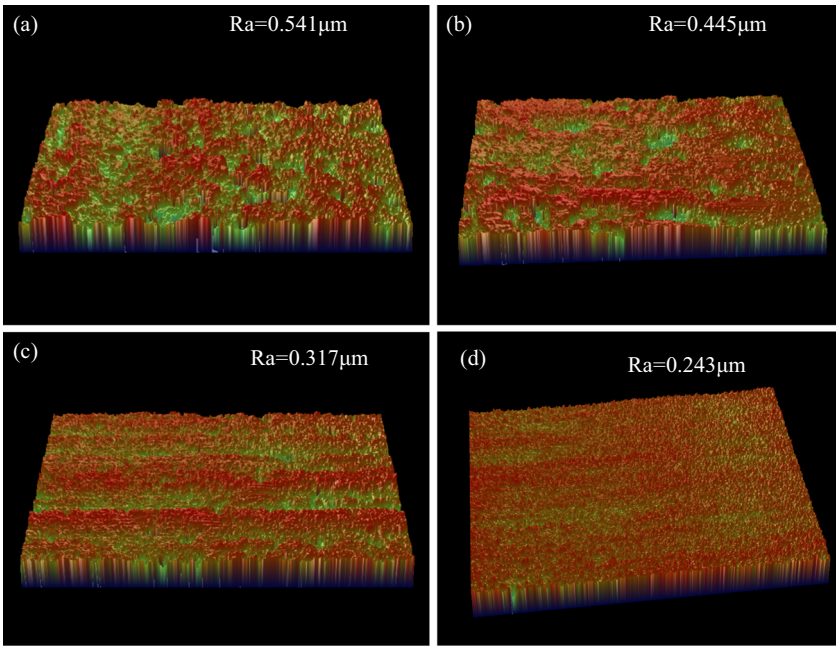

Fig. 10 3D surface roughness characterization by white light interferometer. **a** $v_s = 20$ m/s, $h_{cu} = 1.04$ μm. **b** $v_s = 20$ m/s, $h_{cu} = 0.52$ μm. **c** $v_s = 80$ m/s, $h_{cu} = 1.04$ μm. **d** $v_s = 80$ m/s, $h_{cu} = 0.52$ μm

4 Conclusions

In this paper, a comparative study of high-speed grinding and conventional speed grinding of HIP-silicon carbide ceramics is conducted to investigate the micro-damages and related transformation of microscopic features. Phase transformation, residual stresses, micro-damages, grinding chips, and surface topography have been fully discussed to correlate the grinding surface integrity. The results show that the HSG process could help substantially improve the workpiece integrity in terms of better surface finish, smaller damages, and controlled residual stresses in a higher material removal rate. In high-speed grinding of 80 m/s, the grinding-induced residual stress could be reduced by 30% of conventional grinding of 20 m/s. On the other hand, the grinding damage could be substantially restrained by wheel speed elevation, which is 65 μm of subsurface damage depth at 20 m/s and 14 μm at 80 m/s. In HSG process, the ground surface will be more tended to plastic deformation with less fracture cracks and massive plastic stripes left on the surface. Moreover, it has also been proved that a polytypic phase transformation could be induced in grinding process, which might be the reason of grinding-induced shock temperature and force. From the XRD analysis, it could be concluded that a minor phase transformation happened in high-speed grinding and the 6H-SiC almost stay the same in both grinding modes. Finally, it is suggested to conduct HSG process at a fast workpiece rotational speed to achieve higher material removal rate and better quality control.

Funding information This work is supported in by the China Postdoctoral Science Foundation (2018M630384) and the Fundamental Research Funds for the Central Universities (NO. 2232018D3-14 and 2232018D3-25). The authors wish to record their gratitude for their generous supports.

Compliance with ethical standards

Conflicts of interest The authors declare that they have no conflict of interest.

Publisher's Note Springer Nature remains neutral with regard to jurisdictional claims in published maps and institutional affiliations.

References

1. Liew PJ, Yan J, Kuriyagawa T (2013) Carbon nanofiber assisted micro electro discharge machining of reaction-bonded silicon carbide. J Mater Process Technol 213(7):1076–1087
2. Wang CC, Fang QH, Chen JB, Liu YW, Jin T (2016) Subsurface damage in high-speed grinding of brittle materials considering kinematic characteristics of the grinding process. Int J Adv Manuf Technol 83:937–948
3. Jiang JL, Ge PQ, Bi WB, Zhang L, Wang DX, Zhang Y (2013) 2D/3D ground surface topography modeling considering dressing and wear effects in grinding process. Int J Mach Tool Manu 74:29–40
4. Simanchal K, Bandyopadhyay PP, Paul S (2017) High speed and precision grinding of plasma sprayed oxide ceramic coatings. Ceram Int 43:15316–15331
5. Wang DX, Ge PQ, Bi WB, Jiang JL (2014) Grain trajectory and grain workpiece contact analyses for modeling of grinding force and energy partition. Int J Adv Manuf Technol 70:2111–2123
6. Wu CJ, Li BZ, Yang JG, Liang SY (2016) Prediction of grinding force for brittle materials considering co-existing of ductility and brittleness. Int J Adv Manuf Technol 87:1967–1975
7. Zhang QL, To S, Zhao QL, Guo B (2016) Surface generation mechanism of WC/Co and RB-SiC/Si composites under high spindle speed grinding (HSSG). Int. J Refract Met H Mater 56:123–131
8. Zhu YQ, Sekine T, Kobayashi T, Takazawa E (1998) Shock-induced phase transitions among SiC polytypes. J Mater Sci 33(24):5883–5890

9. Lu YP, He DW, Zhu J, Yang XD (2008) First-principles study of pressure-induced phase transition in silicon carbide. Physica B 403(19–20):3543–3546
10. Dompoint D, Boulle A, Sandulache G, Chaussende D, Hoa LTM, Ouisse T, Eyidi D, Demenet JL, Beaufort MF, Rabier J (2011) Kinetics of the 3C-6H polytypic transition in 3C-SiC single crystals: a diffuse X-ray scattering study. J Appl Phys 110(5):053508
11. Frangulyan TS, Vasilev IP, Ghyngazov SA (2018) Effect of grinding and subsequent thermal annealing on phase composition of subsurface layers of zirconia ceramics. Ceram Int 44(2):2501–2503
12. Dai JB, Ding WF, Zhang LC, Xu JH, Su HH (2015) Understanding the effects of grinding speed and undeformed chip thickness on the chip formation in high-speed grinding. Int J Adv Manuf Technol 81:995–1005
13. Esmaeilzare A, Rahimi A, Rezaei SM (2014) Investigation of subsurface damages and surface roughness in grinding process of Zerodur® glass–ceramic. Appl Surf Sci 313:67–75
14. Liang GX, Schmauder S, Lyu M, Schneider Y, Zhang C, Han Y (2018) An investigation of the influence of initial roughness on the friction and wear behavior of ground surface. Mater 11(2):237
15. Chen SS, Cheung CF, Zhao CY, Zhang FH (2017) Simulated and measured surface roughness in high-speed grinding of silicon carbide wafers. Int J Adv Manuf Technol 91:719–730
16. Ramesh K, Yeo SH, Gowri S, Zhou L (2001) Experimental evaluation of super high-speed grinding of advanced ceramics. Int J Adv Manuf Technol 17:87–92
17. Yin L, Huang H, Ramesh K, Huang T (2005) High speed versus conventional grinding in high removal rate machining of alumina and alumina–titania. Int J Mach Tool Manu 45:897–907
18. King RF, Tabor D (1954) The strength properties and frictional behavior of brittle solids. Proc R Soc London Ser A 223(1153): 225–238
19. Lawn BR, Marshall DB (1979) Hardness, toughness, and brittleness: an indentation analysis. J Am Ceram Soc 62(7–8):347–350
20. Bifano TG, Dow TA, Scattergood RO (1991) Ductile-regime grinding: a new technology for machining brittle materials. J Eng Indus Trans ASME 113(2):184–189
21. Venkatachalam S, Li XP, Liang SY (2009) Predictive modeling of transition undeformed chip thickness in ductile-regime micro-machining of single crystal brittle materials. J Mater Process Technol 209(7):3306–3319
22. Yang M, Li CH, Zhang YB, Jia DZ, Zhang XP, Hou YL, Li RZ, Wang J (2017) Maximum undeformed equivalent chip thickness for ductile-brittle transition of zirconia ceramics under different lubrication conditions. Int J Mach Tool Manu 122:55–65
23. Wu CJ, Li BZ, Liang SY (2016) A critical energy model for brittle-ductile transition in grinding considering wheel speed and chip thickness effects. Proc Inst Mech Eng B-J Eng Manuf 230(8): 1372–1380
24. Muhammad A, Zhang XQ, Mustafizur R, Senthil K (2013) A predictive model of the critical undeformed chip thickness for ductile–brittle transition in nano-machining of brittle materials. Int J Mach Tool Manu 64:114–122
25. Wu CJ, Li BZ, Liu Y, Liang SY (2017) Surface roughness modeling for grinding of silicon carbide ceramics considering co-existing of brittleness and ductility. Int J Mech Sci 133:167–177
26. Liu CJ, Ding WF, Yu TY, Yang CY (2018) Materials removal mechanism in high-speed grinding of particulate reinforced titanium matrix composites. Precis Eng 51:68–77
27. Rowe WB (2014) High-Speed Grinding: Principles of Modern Grinding Technology (Second Edition), Book Chapter, William Andrew. 101–112